PHYSICAL REVIEW B **73**, 081310(R) (2006)

Isolated quantum dot in application to terahertz photon counting

H. Hashiba and V. Antonov
Physics Department, Royal Holloway University of London, Egham, Surrey TW20 0EX, United Kingdom

L. Kulik
Institute of Solid State Physics, RAS, Chernogolovka 142432, Russia

A. Tzalenchuk, P. Kleinschmid, and S. Giblin
National Physical Laboratory, Hampton Road, Teddington, Middlesex TW11 0LW, United Kingdom

S. Komiyama
University of Tokyo, Komaba 3-8-1, Meguro-ku, Tokyo 153-8902, Japan

(Received 21 November 2005; revised manuscript received 27 January 2006; published 21 February 2006)

We present an experimental study of a large quantum dot (QD) capacitively coupled to an aluminum single electron transistor (SET) and irradiated with terahertz radiation from a blackbody source. The SET is used as a noninvasive electrometer sensitive to a single-charge fluctuation on the QD. Qualitatively different regimes of QD confinement have been identified from the SET response. We demonstrate that the state of a nearly isolated QD can potentially be used for counting individual terahertz photons.

DOI: 10.1103/PhysRevB.73.081310 PACS number(s): 73.21.La, 73.23.Hk, 78.67.Hc

The operation range of available single-photon detectors, such as avalanche photodetectors and negative electron affinity photocathode photomultipliers, is limited to the visible and infrared regions.[1,2] To extend photon counting to the gigahertz and terahertz range new counting mechanisms have been suggested. They employ an effect of photoconductive gain in semiconductor field effect transistors (FET) or single electron transistors (SET), in which long-lived nonequilibrium states exist. When a photoexcited electron is trapped in such a state, its electric charge changes the conductivity in the detector source-drain channel. A single photoelectron can govern the current of millions of electrons, creating a huge photoconductive gain. Several types of the photon counting detectors have been reported.[3,4] Having a good sensitivity, the noise equivalent power (NEP) is $\sim 10^{-20}$ W/$\sqrt{\text{Hz}}$, these detectors lack an application feasibility, which is hampered by the necessity of ultralow temperature, high-magnetic field, or fine adjustment of electrostatic gates for operation. A need to tune for the highest sensitivity to the microwave radiation and the highest amplification gain simultaneously is another disadvantage of the reported detectors.

We suggest a more advanced system where a nearly isolated quantum dot (QD) is capacitively coupled to an external SET electrometer. The SET works as a noninvasive probe of the QD charge state. It records events of the photon-assisted electron tunneling from the QD central island to a surrounding electron reservoir, thus enabling a single photon counting. A profound knowledge of the QD is needed for the development of such a detector. In this paper we examine the charge states of a lateral semiconductor QD depending on its coupling to charge reservoirs, the gate potentials and illumination with the terahertz radiation.[5] These help to assess the QD-SET system as a terahertz photon counter.

The QD is defined in a two-dimensional electron gas (2-DEG) formed at depth 90 nm in a GaAs/AlGaAs heterostructure with mobility of 5×10^5 cm/V s and carrier concentration of 2×10^{11} cm^{-2}. The QD is formed as a wet etched mesa stripe of 1 μm width crossed by two negatively biased gates. A cross gate is set at one side of the mesa stripe and a split gate is at the other side, as shown in Fig. 1. The gates form a dipole antenna concentrating the electric field at the QD. An aluminum SET is fabricated on top of the QD. The vertical arrangement of the SET and the QD ensures a large capacitance coupling between them.[6,7] We have performed measurements on a few samples. All showed similar

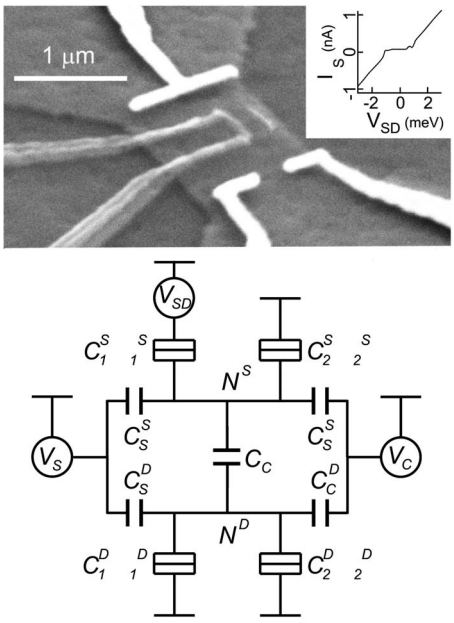

FIG. 1. Scanning electron micrograph of the device. In the inset, *I-V* characteristics of the SET electrometer. Equivalent circuit diagram of the device is shown at the bottom.

behavior, and here we present results from two of them. The measurements are done in a He^3 refrigerator at a temperature of 0.3 K where aluminum is superconducting and the SET is in a regime of Cooper pair tunneling. The SET, with charging energy $E_C = e^2/2C \sim 220\ \mu$eV and total resistance $\sim 2.4\ \mathrm{M}\Omega$, is biased at the Josephson quasiparticle peak, where it has the highest sensitivity. As a broadband terahertz source we use filtered blackbody radiation generated by passing a current through a 5 kΩ resistor. The resistor is sealed in a metal box at the 1 K stage of the refrigerator 50 cm away from the device. A black polyethylene and a Si crystal filter attenuate the high frequency part ($>500\ \mathrm{cm}^{-1}$) of the blackbody radiation. Radiation is fed to the device by a waveguide.

In a classical picture the QD-SET system is modeled as a network of tunnel resistors and capacitors (Fig. 1). The number of electrons on the QD and SET islands are N_D and N_S. The islands are coupled to the cross and split gates with voltages V_C and V_S through capacitances C_C^D, C_C^S, C_S^D, and C_S^S. The islands are connected to the ground and to the source-drain voltage through tunnel barriers represented in the equivalent circuit by resistors and capacitors connected in parallel, Fig. 1. The QD tunnel barriers are governed by the gate voltages V_C and V_S. Increasing the negative voltage bias on the gates reduces the QD tunnel capacitances and increases the tunnel resistances. The QD and the SET are coupled by a capacitance C_C. The offset charges on the QD and the SET are expressed as

$$Q_0^S = (V_S C_S^S + V_C C_C^S) + \frac{C_C(V_S C_S^D + V_C C_C^D - eN_D)}{C_S^D + C_C^D + C_C + C_1^D + C_2^D}, \quad (1)$$

$$Q_0^D = (V_S C_S^D + V_C C_C^D) + \frac{C_C(V_S C_S^S + V_C C_C^S - eN_S)}{C_S^S + C_C^S + C_C + C_1^S + C_2^S}. \quad (2)$$

The split and cross gates adjust the offset charge on the QD and SET. Through the second term in Eq. (1), the SET probes all the capacitances to the QD, and thus provides information about the QD charge state when there is no current through the QD. The latter situation occurs when either of the QD point contacts is pinched off by applying a large negative voltage to the gates. Depending on the QD tunneling regime three different states are observed (see Fig. 2):

(i) One of the QD point contacts is open. In this regime, designated as regime I in Fig. 2, the QD charge is not quantized, and the capacitance of the open contact is so large that the second term of Eq. (1) is negligible. The SET offset charge changes as $Q_0^S = V_S C_S^S + V_C C_C^S$ and current through the SET demonstrates a long period oscillation due to the addition of a Cooper pair to the SET central island. From the oscillation period capacitances between the gates and the SET $C_C^S = C_S^S = 5$ aF are determined.

(ii) Both QD point contacts pinch off the 2DEG channel but one or both of them are set in a weak tunneling regime, region II in Fig. 2. The current through the SET demonstrates an oscillating behavior with two characteristic periods. Long period oscillations, as in regime I, originate from the Coulomb blockade on the SET. Short period oscillations (Fig. 2 inset) are due to charge quantization on the QD island. Variation of the gate biases continuously induces an offset charge on the QD, whereas the number of electrons on the QD island is an integer. The difference between the offset and the integer charge oscillates causing oscillation in Q_0^S through the capacitance C_C [the second term in Eq. (1)]. At each peak the average charge on the island changes by one electron; between peaks the number of electrons on the island remains constant. In our experimental design N^D changes by more than 10 before N^S changes by 1. Any SET feedback to the dot can therefore be neglected, and the SET thus forms a noninvasive electrometer of the dot-charge state. From the QD Coulomb blockade oscillations the capacitances $C_S^D = 80$ aF and $C_C^D = 60$ aF between the QD island and the split and cross gates are determined. Removing an electron from the QD island causes a shift of $e(C_C/C_\Sigma)$ in the SET offset charge, where $C_\Sigma = C_S^D + C_C^D + C_C + C_1^D + C_2^D$. Thus, from the amplitude of the short oscillation period the ratio C_C/C_Σ is determined. The amplitude increases towards a more negative gate bias when the capacitance coupling between the QD island and the surrounding electron reservoir reduces. Also charge quantization conditions improve with increasing the tunnel resistances. Close to the pinch-off regime the amplitude corresponds to $\sim 0.1e$.

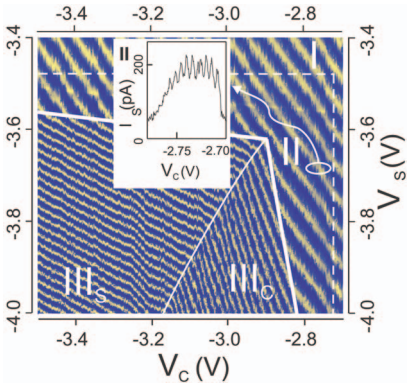

FIG. 2. Image of the SET-current vs biases on split and cross gates. Thick white lines indicate pinch-off boundary. Thin line indicates the "leaking" area boundary. Dashed lines point out the area of QD charge quantization oscillations. An example of the oscillations is shown in the inset.

(iii) Both quantum point contacts are pinched off. Electrons cannot escape from the QD island during the gate sweep leaving the island in a nonequilibrium state with respect to the surrounding electron reservoir. Here, the physics of the completely isolated quantum dot is directly accessed. Since the capacitances between the gates and the QD island are significantly larger than those between the gates and the SET, the SET Coulomb blockade oscillations abruptly shrink in period at the pinch-off boundary separating equilibrium II and nonequilibrium III states. The effective capacitances between the gates and the SET increase to $C_{C,S}^S + C_C C_{C,S}^D / C_\Sigma$. This regime, where N_D is constant, is denoted III$_S$ in Fig. 2.

Subsequent ramping of the gates inside the pinch-off area transfers the QD to a new state characterized by a large number of random switching events. The phase and amplitude

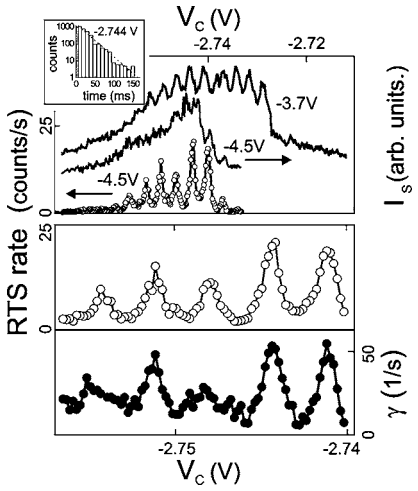

FIG. 3. Top: SET current in area II and at the pinch-off boundary. The random telegraph signal rate is also shown. In the inset, an example of statistics for intervals between single-electron tunneling events. The exponential decay is consistent with thermoactivation origin of the RTS. Bottom: RTS rate and reciprocal lifetime of the excited state vs gate bias.

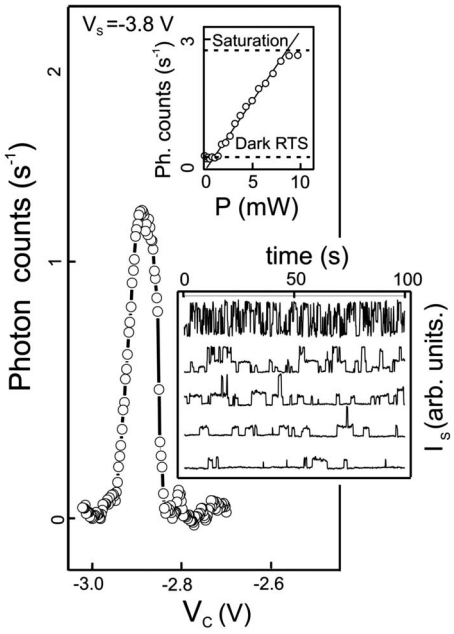

FIG. 4. Detector photoresponse vs cross-gate bias measured with integration constant 100 ms. The bottom inset shows time traces of photoinduced RTS at different emitter powers (increased from bottom to top). With increasing the power-level time, traces with rare individual switches between the ground and the first QD excited states transform to traces with rapid switching between the ground and multiple excited QD states. The top inset shows the dependence of the photon counting signal on the integral power level emitted by the resistor. The dark RTS and the detector saturation level are shown by the dashed lines.

analysis indicates that most of them correspond to a single-electron tunneling off the QD. We conclude that in this regime, denoted III_C, further increases in the confining potential barrier squeeze electrons out of the QD. The position of the boundary dividing regions III_C and III_S is dependent on the number of electrons trapped in the QD when the II-III_C boundary is crossed. It thus depends on the history of the gate voltages. Figure 2 was obtained by sweeping V_S at constant V_C, but if V_C is swept, regions III_C and III_S change places.

Regimes I, II, and III_S are important for finding the system parameters (capacitances to the gates, shunt, and total capacitances of the QD and the SET). Analysis of the "leaky" state III_C provides a direct experimental probe for the potential barrier formation in the QD. Assuming the number of nonequilibrium electrons trapped in the QD is linearly proportional to the electrochemical potential, one can draw the barrier height as function of the corresponding gate bias.[8]

In application to photon detection, the working point should be chosen close to the pinch-off boundary separating areas II and III in such a way that the lifetime of QD excited states would be consistent with the desired detector dynamic range and the bandwidth of the SET current measurement electronics. It is an easy task as a large number of random telegraph switches of the SET current are observed at certain gate biases. They cause smearing of the short period oscillations, Fig. 3. This indicates that thermally activated electron tunneling on and off the QD island occurs within the time domain of the instrumental time constant.[9] The random telegraph signal (RTS) rate varies periodically with the applied gate bias. The latter variations arise from changes in the tunneling rate between the electron energy levels in the QD island and the conducting leads, and have the same periodicity as the QD charge quantization oscillations in the SET current. The peaks in the RTS rate correspond to charge degeneracy points at which the QD charge changes from N to $N+1$. The electron number at the degeneracy points is fluctuating between two quantized values.

The photoresponse appears as an increase of the RTS rate over the equilibrium and noise switching rate after illuminating the device with terahertz radiation (see Fig. 4). The sample is identical to that discussed above. The equilibrium and noise switchings are suppressed below $V_C \sim -2.85$ V to the level of 0.2 counts/s. The rate of photon assisted switchings remains high up to $V_C \sim -2.95$ V. The switching rate saturates with an increase of the power applied to the emitter due to the measurement setup integration time constant $\tau \sim 0.1$ s (there should be at least three points per one count, which makes the maximum count rate about 3 counts/s).

The photoresponse mechanism can be understood as follows[4]: A terahertz photon excites resonantly a plasma mode in the QD island that has a finite probability to decay in single-particle excitations outside the island if the potential barriers confining the QD are not too high. If this event occurs, the negative charge on the island is temporarily reduced until it is repopulated by an electron tunneling onto the island. This results in a temporary change to the potential of the QD, which causes an observable rise or reduction in the SET tunnel current depending on the phase of the SET Coulomb blockade oscillation at the working point. When the photon flux increases, double, triple, and higher order excited states, with correspondingly shorter lifetimes, are observed (see Fig. 4).[3]

We estimate the noise equivalent power of the detector using $\mathrm{NEP}=hf\eta^{-1}\sqrt{2N_{RTS}}$, where f, η, and N_{RTS} are the frequency rate, quantum efficiency rate, and dark RTS rate, respectively.[10] We refer to Ref. 11, where estimation of the quantum efficiency in a similar system has been addressed. In the calculation, a few factors were considered: (i) dissipation within antenna, (ii) coupling of the antenna to free space, and (iii) impedance matching of the antenna with the QD. The quantum efficiency of 1% is a fair estimation. Using this number we get $\mathrm{NEP}\sim 10^{-19}$ W/$\sqrt{\mathrm{Hz}}$, which is superior to any bolometers in this frequency range. Notice that the sensitivity changes by about one order, depending on whether the detector working point is chosen close to the split-gate pinch-off boundary or to the cross-gate one. This phenomenon is related to the probability of the QD plasma mode to decay outside the QD island through the potential barrier separating the island and the corresponding lead. It is larger for the ridge-shaped cross-gate potential than for the saddle-shaped split-gate potential as an electron must tunnel off the island mainly through the thin valley of the split gate. See the corresponding pinch-off biases in Fig. 2.

This work is supported by the Solution Oriented Research for Science and Technology (SORST) from Japan Science and Technology (JST), and the National Measurement System Policy Unit of the Department of Trade and Industry, U K. L.K. acknowledges support of the Royal Society for his short visit to the United Kingdom.

[1] K. M. Johnson, IEEE Trans. Electron Devices **12**, 55 (1965).
[2] R. L. Bell, *Negative Electron Affinity Devices* (Clarendon, Oxford, England, 1973) p. 64.
[3] S. Komiyama, O. Astafiev, V. Antonov, T. Kutsuwa, and H. Hirai, Nature (London) **403**, 405 (2000).
[4] J. M. Hergenrother, J. G. Lu, M. T. Tuominen, D. C. Ralph, and M. Tinkham, Phys. Rev. B **51**, 9407 (1995); A. Cleland, D. Esteve, C. Urbina, and M. Devoret, Appl. Phys. Lett. **61**, 2820 (1992); H. Hashiba, V. Antonov, L. Kulik, S. Komiyama, and C. Stanley, *ibid.* **85**, 6036 (2004).
[5] L. I. Glazman and K. A. Matveev, Zh. Eksp. Teor. Fiz. **98**, 1834 (1990) [JETP **71**, 1031 (1990)]; K. A. Matveev, Phys. Rev. B **51**, 1743 (1995).
[6] M. Koltonyuk, D. Berman, N. B. Zhitenev, R. C. Ashoori, L. N. Pfeiffer, and K. W. West, Appl. Phys. Lett. **74**, 555 (1999).
[7] W. Lu, A. J. Rimberg, K. D. Maranowski, and A. C. Gossard, Appl. Phys. Lett. **77**, 2746 (2000).
[8] J. Martorell, D. W. L. Sprung, P. Machado, and C. G. Smith, Phys. Rev. B **63**, 045325 (2001).
[9] W. Lu, Z. Ji, L. Pfeiffer, K. W. West, and A. J. Rimberg, Nature (London) **423**, 422 (2003).
[10] P. L. Richards, J. Appl. Phys. **76**, 1 (1994).
[11] O. Astafiev, S. Komiyama, T. Kutsuwa, V. Antonov, Y. Kawaguchi, and K. Hirakawa, Appl. Phys. Lett. **80**, 4250 (2002).